ELSEVIER

Polymer 42 (2001) 8935–8946

polymer

www.elsevier.com/locate/polymer

Dimensions of polyelectrolyte chains and concentration fluctuations in semidilute solutions of sodium–poly(styrene sulfonate) as measured by small-angle neutron scattering

V.M. Prabhu[a], M. Muthukumar[a,*], G.D. Wignall[b], Y.B. Melnichenko[b]

[a]*Department of Polymer Science and Engineering, Materials Research Science and Engineering Center, University of Massachusetts, Amherst, MA 01003, USA*

[b]*Oak Ridge National Laboratory, Solid State Division, Oak Ridge, TN 37831-6393, USA*

The authors consider it an honor to contribute to a celebration dedicated to Richard Stein, both on account of personal friendship and inspiration for SANS

Received 28 February 2001; received in revised form 12 March 2001; accepted 12 March 2001

Abstract

We have measured the radius of gyration (R_g) of labeled polymer chains and the correlation length (ξ) for semidilute solutions of sodium–poly(styrene sulfonate) using small-angle neutron scattering (SANS). This is the first measurement of both length scales as the system is advanced to an unstable phase boundary by adding barium chloride salt. The R_g decreases from 80 ± 2 to 54 ± 2Å as the salt concentration is increased. Simultaneously, ξ is found to crossover from $\xi \ll R_g$ to $\xi \gg R_g$. This crossover signals the enhancement of concentration fluctuations. In addition to extracting these length scales a crossover from mean-field to Ising criticality is observed. This conclusion is made within the context of a mean-field model, which supports temperature and salt-induced phase separation.

Keywords: Sodium–poly(styrene sulfonate); Polyelectrolytes; Semidilute solutions

1. Introduction

In polymeric mixtures, χN determines the state of miscibility, where χ is the Flory–Huggins interaction parameter, typically proportional to inverse temperature and N the degree of polymerization. The connectivity of the monomers leads to molecular weight controlling the miscibility in an equivalent manner as inverse temperature. Due to this fact, uncharged model polymer mixtures have been extensively investigated to explore the critical exponents, experimental ranges of dominance of concentration fluctuations, and the nature of the crossover from the mean-field to Ising behaviors [1]. On the other hand, there has been little experimental study on critical phenomena of polyelectrolyte solutions, where the potential interactions among monomers are long-ranged. In such systems with long-range interactions, even the nature of the universality class is not known. In addition to molecular weight, the range of electrostatic interaction is an important variable in dictating the phase behavior of polyelectrolyte solutions.

In an effort to explore the phase behavior of polyelectrolyte solutions, we have studied experimentally, solutions of sodium–poly(styrene sulfonate) in water at different ionic strengths by controlling the amounts of added barium chloride. First, we have identified the salting out phase boundaries for a given temperature as a function of added salt. We have then investigated using small-angle neutron scattering (SANS) the radius of gyration (R_g) of labeled polymers, the correlation length (ξ) of concentration fluctuations, and the osmotic compressibility ($\sim I(0)$, scattered intensity at zero-angle) in the homogeneous phase as the unstable phase boundary is approached by adding barium chloride.

In this paper, we focus only on the apparent critical behaviors of the system due to added salt at a fixed temperature. By considering the influence of added salt ions and counter-ions of the polyelectrolyte in terms of a Debye length (κ^{-1}) [2], our SANS data show that ξ and $I(0)$ diverge as the phase boundary is approached. The divergence is quantified as a crossover from mean-field to Ising criticality, close to the salt-induced phase boundary. The divergence is made with respect to a critical inverse-square Debye length κ_c^2. The solution thermodynamics is examined by a mean-field theory.

* Corresponding author. Tel.: +1-413-577-1212; fax: +1-413-545-0082.
E-mail address: muthu@polysci.umass.edu (M. Muthukumar).

0032-3861/01/$ - see front matter
PII: S0032-3861(01)00382-2

The rest of the paper is organized as follows: Section 2 contains relevant theoretical preliminaries and Section 3 describes our experimental protocols. Our results and their discussion are presented in Section 4 before concluding in Section 5.

2. Theoretical preliminaries

The present experimental problem is one of a multi-component solution. In order to bring some physical understanding of the essential physics for this system, we have taken the multi-component solution as a quasi two-component system consisting of the polymer and an effective solvent. The influence of the added electrolytes is captured by the Debye length associated with the solvent. In the presence of a bathing electrically neutral ionic medium, the bare Coulomb interaction between two point charges separated by a distance r becomes screened and takes on the Debye–Hückel form [2].

Our model [3] for understanding the monomer–monomer correlations begins with the potential, $V(r)$, between Kuhn segments,

$$\frac{V(r)}{k_B T} = w\delta(r) + w_c l_k^3 \frac{e^{-\kappa r}}{r}. \tag{1}$$

The first term is the short-ranged excluded-volume pseudo-potential and the second term the long-ranged electrostatic contribution. w represents the pseudo-potential strength and is equivalent to $(1/2 - \chi)l_k^3$, where χ is the Flory–Huggins interaction parameter, which describes the chemical mismatch between monomer and solvent for neutral solutions. l_k is the Kuhn statistical segment length. $\delta(r)$ is the Dirac delta function. The strength w_c is a result of modeling the polymer with a uniform charge, where each monomer is treated as a point-like object,

$$w_c = \frac{4\pi Z^2 \alpha^2 l_B}{l_k^3}, \tag{2}$$

where Z is the Kuhn segment valence, α the degree of ionization, and the Bjerrum length l_B is given by $e^2/4\pi\epsilon\epsilon_0 k_B T$. e is the electronic charge, ϵ and ϵ_0 the solvent dielectric constant and permittivity, respectively. Knowing the monomer valence, one can scale the theoretical valence of the Kuhn segment by the ratio of Kuhn length to monomeric contour length.

Within the Debye–Hückel approximation, the dominant range of the interaction is dictated by the inverse-square Debye length κ^2,

$$\kappa^2 = 4\pi l_B N_A 1000 \left(Z_c^2 \alpha C_c + \sum_\gamma Z_\gamma^2 C_\gamma \right), \tag{3}$$

where N_A is Avogadro's number, Z_c and C_c the counter-ion valence and concentration, respectively ($C_c = C_m$, the monomer concentration). Z_γ and C_γ are the added salt valence and concentration, respectively, of the γ added salt ion. We have introduced the influence of the polymer counter-ions to the total solution ionic strength. This is motivated by including all randomly distributed ions, which may include a fraction (αC_c) of dissociated counter-ion species. Within this description the only measure for polymer–salt interactions, such as counter-ion condensation and dissociation equilibria are parameterized by a degree of ionization of the chain through α. The concentrations C_c and C_γ are in molar units.

Upon Fourier transform of the model potential and in the limit of high salt, such that $\kappa^2 \gg \mathbf{q}^2$, where $\mathbf{q}$ is the scattering wavevector, the model potential becomes short-ranged [3,4] and only modifies the strength of the pseudo-potential w. As a direct consequence of the high salt limit, the Flory–Huggins interaction parameter is modified such that,

$$(1/2 - \chi) \rightarrow (1/2 - \chi_0) + \frac{w_c}{\kappa^2}. \tag{4}$$

The new Flory–Huggins interaction parameter (χ_{Eff}) is composed of a neutral chemical mismatch (χ_0, related exactly to the pseudo-potential strength w) between monomer and solvent and an electrostatic contribution, which is a function of the ionic strength (w_c/κ^2),

$$\chi_{Eff} = \chi_0 - \frac{w_c}{\kappa^2}. \tag{5}$$

χ_0 is a function of temperature, usually of the form $A/T + B$ and the electrostatic term is athermal. Thus, the temperature dependence and ionic strength dependence are separated.

In general, the structure factor ($S_t(\mathbf{q})$) measured in a total scattering experiment is the Fourier transform of the pair-correlation function [5]. The final form of the general scattering equation in terms of the absolute differential coherent neutron scattering cross-section, $I(\mathbf{q})$, is,

$$I(\mathbf{q}) = \left(\frac{b^2}{v_m} \right) S_t(\mathbf{q}), \tag{6}$$

$$b = \left(b_m - \bar{b}_s \frac{v_m}{v_s} \right). \tag{7}$$

This form chooses the molecular volume of the monomer, v_m, as the reference volume. b is the contrast factor, defined by Eq. (7), b_m the coherent scattering length of the monomeric anion, $\bar{b}_s$ the average coherent scattering length of the solvent, which includes the monomer counter-ions and added salt ions, and v_s the molecular volume of the solvent.

Using the main results of the random phase approximation (RPA) [3,5–11] for the effective two-component system, the form for the structure factor is,

$$S_t(\mathbf{q})^{-1} = \frac{1}{\phi S_D(\mathbf{q})} + \frac{1}{1 - \phi} - 2\chi_{Eff}, \tag{8}$$

where ϕ is the polymer volume fraction and $S_D(k)$ the Debye structure factor. We then introduce the effective Flory–Huggins interaction parameter, Eq. (5), and use the Debye

structure factor in $\mathbf{q}R_g < 1$ limit. The result is,

$$S_t(\mathbf{q})^{-1} = \frac{1}{\phi N} + \frac{1}{1-\phi} - 2\chi_0 + \frac{\mathbf{q}^2 R_g^2}{3\phi N} + \frac{2w_c}{\kappa^2}. \quad (9)$$

This formula reproduces the Ornstein–Zernicke form,

$$S_t(\mathbf{q})^{-1} = A[\kappa^2][1 + \xi^2\mathbf{q}^2],$$

$$A[\kappa^2] = \frac{1}{\phi N} + \frac{1}{1-\phi} - 2\chi_0 + \frac{2w_c}{\kappa^2}, \quad (10)$$

$$\xi^2 = \frac{R_g^2/3\phi N}{A[\kappa^2]}.$$

Thus, one may extract the correlation length (ξ) and scattered intensity to zero angle ($I(0)$) from the Ornstein–Zernicke plot. In the limit of $\mathbf{q} = 0$, χ_0 and w_c are determined. This is achieved by inspecting the linear equation in $1/\kappa^2$, after substitution of Eq. (10) into the general expression Eq. (6),

$$I(\mathbf{q}=0)^{-1}\left(\frac{b^2}{v_m}\right) - \left(\frac{1}{\phi N} + \frac{1}{1-\phi}\right) = -2\chi_0 + \frac{2w_c}{\kappa^2}. \quad (11)$$

2.1. Relation to critical phenomena

As discussed in Section 1, our understanding of the universality class of polyelectrolyte solutions is limited. We will illustrate using the mean-field model that one may experimentally observe a unique situation of salt-induced criticality. Returning to the neutral polymer case RPA predicts the correlation length to diverge,

$$\xi^2 \sim A[T]^{-1},$$

where,

$$A = \frac{1}{\phi N} + \frac{1}{1-\phi} - 2\chi_0, \quad (12)$$

$$A \sim 2(\chi_s - \chi_0) \sim \left(\frac{1}{T_s} - \frac{1}{T}\right), \quad (13)$$

where χ_s is value of the Flory–Huggins interaction parameter at the spinodal temperature. As the system is brought closer to the spinodal curve by lowering temperature, ξ and $I(0)$ diverge with mean-field critical indices of $\nu = 0.5$ and $\gamma = 1.0$ [12].

$$\xi^{-2} \sim \left(\frac{1}{T_s} - \frac{1}{T}\right)^{2\nu} \quad \text{and} \quad I(0)^{-1} \sim \left(\frac{1}{T_s} - \frac{1}{T}\right)^{\gamma}. \quad (14)$$

However, very close to the critical temperature the critical indices take on the values of the three-dimensional Ising model: $\nu = 0.63$ and $\gamma = 1.24$ [12]. This crossover is observed as a deviation from the linear mean-field plot of ξ^{-2} (or $I(0)^{-1}$) versus $1/T$ where the slope is negative.

In the presented mean-field model for polyelectrolyte solutions, the Flory–Huggins interaction parameter becomes modified as given in Eq. (5), such that,

$$A = 2\left(\chi_s - \chi_0 + \frac{w_c}{\kappa^2}\right) \sim \left(\frac{1}{T_s} - \frac{1}{T} + \frac{w_c}{\kappa^2}\right). \quad (15)$$

Upon replacing the expected temperature dependence for χ_0 and χ_s with $1/T$ and $1/T_s$, respectively, we ignore dimensional prefactors to illustrate the dominant variables. Given the expression for A,

$$\xi^{-2} \sim \left(\frac{1}{T_s} - \frac{1}{T} + \frac{w_c}{\kappa^2}\right)^{2\nu} \quad \text{and}$$
$$I(0)^{-1} \sim \left(\frac{1}{T_s} - \frac{1}{T} + \frac{w_c}{\kappa^2}\right)^{\gamma}. \quad (16)$$

Thus, in this case, a plot of ξ^{-2} (or $I(0)^{-1}$) versus $1/\kappa^2$ will yield a straight line with a positive slope. Any deviation near the phase transition may be attributed to the crossover to the Ising universality class. This is the expected behavior in the limit of high salt where the electrostatic interactions become short-ranged.

The above theoretical arguments will be used to provide a minimal quantitative measure for the solution behavior and to understand the universality class of high-salt polyelectrolyte solutions.

2.2. Theory of high concentration labeling

The high concentration labeling method [13,14] has been used to follow single chain scattering for neutral polymeric systems, such as polymer/solvent [15,16], polymer/polymer [17], and polymer/supercritical CO_2 [18] mixtures. Here, we apply the same formalism for aqueous polyelectrolyte solutions. Due to the dominant neutron scattering contrast arising between monomer and solvent concentration fluctuations, the multi-component solution may be treated as an effective two-component system. This two component approximation has been successfully employed for sodium–poly(styrene sulfonate) without added salt [19–21] and with added salt [22].

We refer to the main results of the high concentration methodology for the two component solutions,

$$I(\mathbf{q}) = I_s(\mathbf{q}) + I_t(\mathbf{q}), \quad (17)$$

$$I_s(\mathbf{q}) = KnN^2 S_s(\mathbf{q}), \quad (18)$$

$$I_t(\mathbf{q}) = LnN^2 S_t(\mathbf{q}). \quad (19)$$

The prefactors are

$$K = [b_h - b_d]^2 x_h(1 - x_h),$$

$$L = [b_h x_h + b_d(1 - x_h) - b_s']^2.$$

The absolute differential coherent scattering cross-section, $I(\mathbf{q})$, units of cm^{-1}, in this method is

composed of a sum of two types of scattering; scattering associated with intra-chain monomer–monomer correlations (I_s) and total scattering from all monomer–monomer correlations (I_t), both intra and inter-chain. b_h and b_d are the scattering lengths of the protonated and deuterated monomers, respectively. b'_s is the scattering length of a solvent normalized via the ratio of the specific volume of the monomer and solvent molecule. b'_s may be adjusted by varying average scattering length of the solvent, by using a H_2O and D_2O mixture such that $b'_s = y_h b_{H_2O} + (1 - y_h) b_{D_2O}$, where y_h is the mole fraction of H_2O and b_{H_2O} and b_{D_2O} the scattering lengths. n is the number of polymer molecules per unit volume of solution and N the degree of polymerization. The essential physics remains in the single-chain structure factor (S_s), and the total scattering structure factor (S_t). The single chain scattering may be directly measured by making the prefactor L to the intensity of total scattering go to zero. We will refer to the matching point as the condition such that the average scattering length density [23] of the monomer matches that of the solvent, which gives $L = 0$.

3. Experimental

The sodium–poly(styrene sulfonate) used in this study was prepared via sulfonation of protonated (H-PS) and deuterated (D-PS) polystyrene purchased from Polymer Laboratories and Polymer Source, respectively. These polystyrene standards were characterized by the manufacturers by gel permeation chromatography in tetrahydrofuran. Molecular weight details are given in Table 1. The sulfonation method of Vink [24] was used with modification. The mass of polystyrene used was 400 and 800 mg for the protonated and deuterated reactions, respectively, the phosphorous pentoxide amount was increased by 50% as suggested by Smisek and Hoagland [25], and the amount of crushed ice required to precipitate the polymer was increased to 40 g. The sulfonated polymer, recovered in de-ionized water, was titrated to a pH of 10 using sodium hydroxide solution purchased from Fisher Scientific, certified 0.201-0.199N, and subsequently filtered through a 0.22 μm cellulose acetate filter unit manufactured by Corning Costar. This clear solution was then dialyzed using Spectra/Por molecular-porous membrane tubing with molecular weight cut-off 3500 against water purified by a Milli-Q UF Plus system, a product of the Millipore Corporation, with resistivity 18 MΩ cm. Dialysis was performed with frequent change in the dialysis water. Once the conductance of the dialysis water remained constant over a 24 h period and was below 0.6 μS/cm the solutions were lyophillized. The lyophillized samples were characterized by elemental analysis for sulfur content and agarose gel electrophoresis. Gel electrophoresis was performed using a standard horizontal electrophoresis cell using sodium–poly(styrene sulfonate) from a Scientific Polymer Products Calibration Kit as mobility standards. Seakem LE Agarose of gel electrophoresis quality, distributed by FML Bioproducts, was used at a concentration of 0.9%, the balance buffer solution. The buffer solution used for gel setting as well as recirculating fluid was 0.01 M reagent quality Na_2HPO_4. After electrophoresis with an applied field strength of 2 V/cm for 2 h, the gel was stained with 0.01% methylene blue dye, destained with de-ionized water, and subsequently transferred to a flatbed scanner and digitized for analysis. The digitized bands were analyzed for the peak in the distribution and second moment, from which the polydispersity was obtained [26]. The results are given in Table 1.

Table 1
Polymer characteristics

	H-PS	D-PS	H-NaPSS	D-NaPSS
M_n	29 800	28 500	52 400	54 900
Polymerization degree	287	274	287	274
PDI	1.02	1.03	1.1	1.1
% sulfonation			96	92

Even after exhaustive drying of samples under high vacuum at 80°C, or heating for removal of water in an oven at 105°C, water was observed by thermal-gravimetric analysis. We find an average of 8% by mass of water content through our sample preparation.

The deuterium oxide used in this study, D_2O, was from Cambridge Isotope Laboratories (99.9%) and the water, H_2O, used in this study was of Milli-Q UF Plus System quality with resistivity of 18 MΩ cm. The $BaCl_2$ salt used in this study is a di-hydrate ($BaCl_2 \cdot 2H_2O$) under ambient conditions, but was dried to remove water by heating to 140°C for 24 h.

A single polymer concentration of 202.5 g l^{-1} (per liter of added solvent) was studied. Samples were prepared by mixing dried polymer with the appropriate solvent mixture. We have experimentally determined the matching point condition to extract the single chain scattering, based of the high concentration methodology. In order to make $L = 0$ and yet retain a significant signal-to-noise ratio, we have chosen to fix the fraction of protonated chains at $x_h = 0.4$ and tune the average scattering length of the mixed (H_2O, D_2O) solvent in such a way that $0.4b_h + 0.6b_d = b'_s$. The matching point utilizes a mass fraction of protonated chains, denoted x_h, of 0.40, with solvent of volume fraction H_2O, y_h, of 0.32. To accurately investigate varying salt concentrations, several stock salt solutions were prepared by dilution of a parent salty solution of 0.5 M $BaCl_2$ with $y_h = 0.32$. The absolute matching point conditions are increased to $y_h = 0.33$ due to aforementioned water content. Samples for total scattering measurements were prepared similarly, using D_2O salty solutions and protonated polymer to maximize the scattering contrast.

The experiments were performed on the W.C. Koehler SANS facility at the Oak Ridge National Laboratory [27]. The neutron wavelength was 4.75 Å ($\Delta\lambda/\lambda \approx 5\%$). The sample–detector distance was 5.8 m and the data were

corrected for instrumental backgrounds and detector efficiency on a cell-by-cell basis, prior to radial averaging to give a **q**-range of $0.008 < \mathbf{q} < 0.1$ Å. The net intensities were converted to an absolute (±4%) differential cross-section per unit sample volume (in units of cm^{-1}) by comparison with pre-calibrated secondary standards, based on the measurement of beam flux, vanadium incoherent cross-section, the scattering from water and other reference materials [28]. The efficiency calibration was based on the scattering from light water and this led to angle-independent scattering for vanadium, H-polymer blanks and water samples of different thicknesses in the range 1–10 mm. Procedures for calculating the incoherent background, arising largely from the protons in the sample, have been described previously [29].

4. Results and discussion

We have demonstrated a precipitation map on a plot of added barium chloride salt versus monomer concentration as shown in Fig. 1. Such precipitation diagrams have been observed for many polyelectrolyte and salt systems [11,30–32]. The first observation for precipitation of the sodium–poly(styrene sulfonate)/barium chloride system was made by Narh and Keller [33]. The region of two phases and a stable homogeneous phase are shown. Two distinctly different boundaries between the one and two-phase regions are illustrated in the figure. The first is where the salt concentration is a constant and independent of the added polymer concentration. This limit holds between the range studied of monomer concentration 0.00078–0.0125 M for an added salt concentration of 0.0156 M. The second limit, a linear relation between the monomer and salt concentration is between the polymer concentrations 0.05–1.0 M and salt concentrations 0.0312–0.3375 M, respectively. The transition between the two salting out limits occurs at a ratio of monomer to salt concentration of 1.06. The key issue in this study is to monitor the two different length scales R_g and ξ as a semidilute solution is varied to approach the salting out unstable phase boundary, as follows.

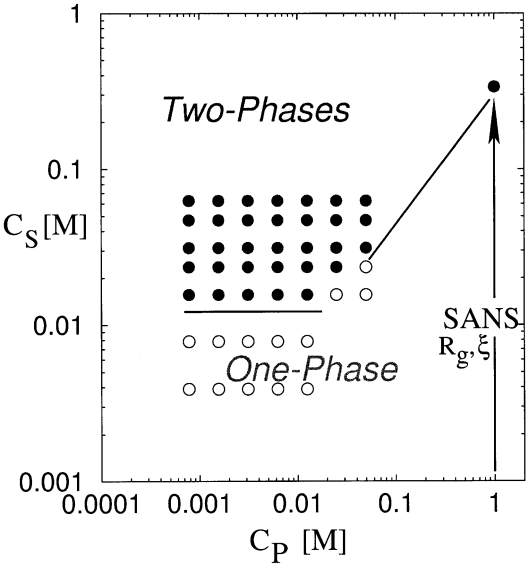

Fig. 1. Precipitation diagram of barium chloride/Na–poly(styrene sulfonate) system.

4.1. High concentration labeling

The *Z*-averaged radius of gyration (R_g) was obtained from fits to the Debye structure factor, $S_D(\mathbf{q})$, Eq. (20), for all 10 salt concentrations investigated,

$$S_D(\mathbf{q}) = \frac{2}{\mathbf{q}^4 R_g^4}(e^{-\mathbf{q}^2 R_g^2} - 1 + \mathbf{q}^2 R_g^2). \quad (20)$$

The method of data fitting was performed with the non-linear regression package from Mathematica 3.0 using the weights from the experimental errors in the measured $I(\mathbf{q})$. A flat incoherent-scattering background was estimated from the scattering by a protonated polymer in the identical D_2O/H_2O mixture. This estimated background at high wave-vectors is 0.341 cm^{-1} and was subtracted from all data sets prior to fitting. Thus, the fitting was to Eq. (18) where S_s is given by Eq. (20). This analysis works well as nearly the entire wavevector range may be fit. Particular exceptions may be made for the three highest salt concentrations where the scattering tends to deviate at low wave-vectors, to obtain good fits the first five data points were not fit. The experimental origin for this deviation may be twofold: (1) these data are of low statistics due to averaging over less than nine detector pixels and (2) there remains a finite contribution from the total scattering. All the data-fits are shown in Fig. 2 and main results tabulated in Table 3. The R_g for varying salt concentration is shown in Fig. 3.

The size of the labeled chains decreases from 80 ± 2 to 54 ± 1 Å when the salt concentration is increased from 0.0 to 0.3375 M. This is a decrease in the size of labeled chains by 33%. The coil shrinkage is consistent with the increased screening of repulsive intra-chain monomer–monomer electrostatic interactions by the mediating ions as the Debye length decreases from 9.57 to 3.04 Å (taking the degree of ionization to be 0.21 as discussed in Section 4.2.1).

To gain an understanding of the size of the labeled chains we compare to the rod-like limit and unperturbed θ-coil dimensions. The measured radius of gyration, with no added salt, is smaller than that of a calculated fully extended rod-like conformation, which is on the order of 200 Å. Thus, in comparison, the experimental data are not properly described by a fully rigid rod-like conformation, even in low ionic strength dilute solutions. The approach to the semi-dilute and concentrated solutions leads to an increased excluded volume screening by the presence of other monomers and electrostatic screening by the presence of dissociated counter-ions, explaining the smaller chain dimensions as theoretically predicted by Muthukumar [3,8].

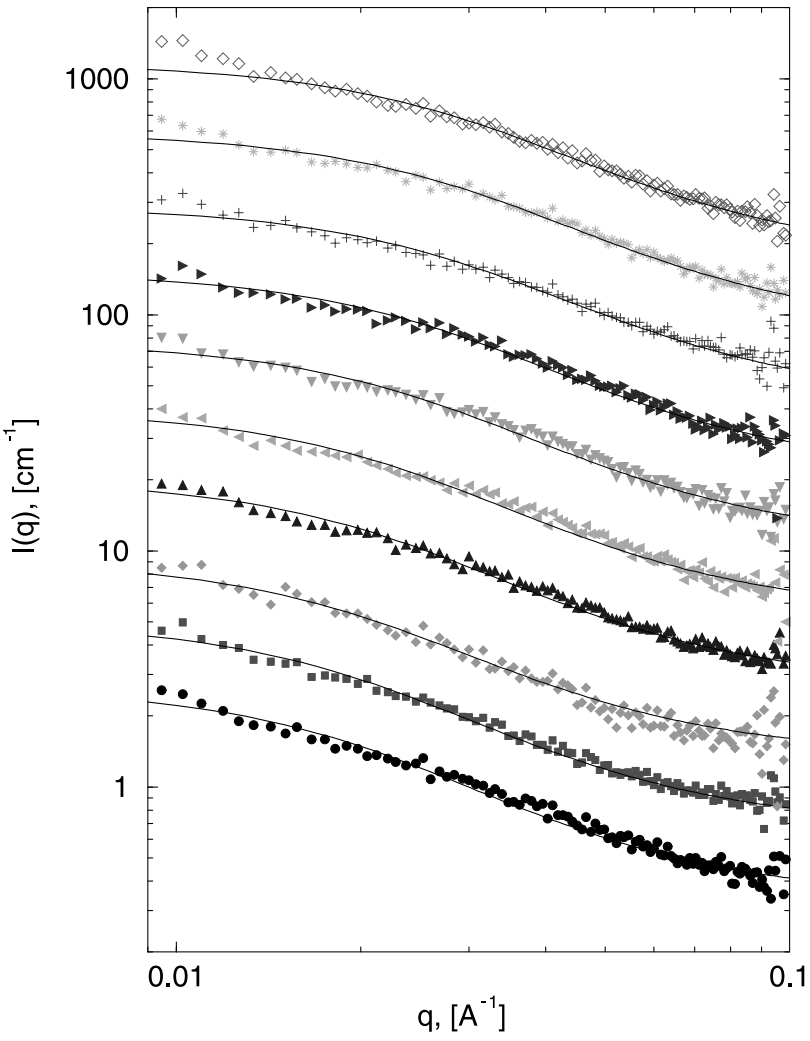

Fig. 2. High concentration labeling, experimental data fit with the Debye structure factor. Data sets are vertically shifted by a factor of 2 for increasing levels of barium chloride salt.

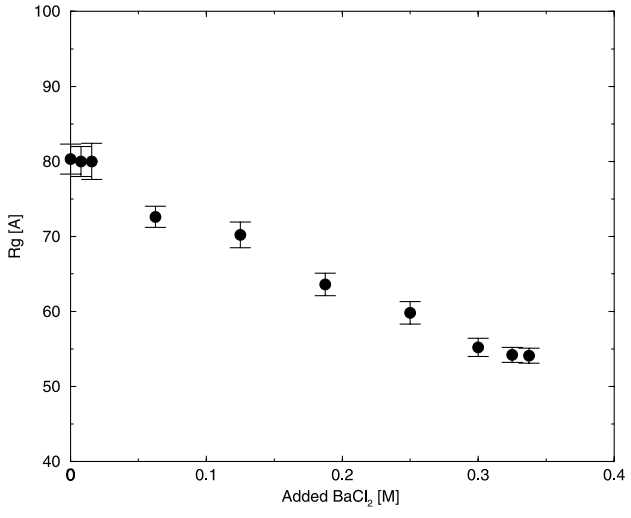

Fig. 3. High concentration labeling, radius of gyration versus added barium chloride salt concentration.

The measured R_g of 54 Å, at the highest salt concentration is larger than the θ-dimensions calculated for fully sulfonated sodium–poly(styrene sulfonate) and polystyrene. Hirose et al. [34] have determined an empirical law of $\langle R_g^2 \rangle_z = 0.030$ Å^2 M_W under experimental θ-solvent conditions from dilute solution light scattering at 4.17 M NaCl and 16.4°C. This law calculates a z-average radius of gyration of 42.2 Å for our system using a weight average molecular weight as $(0.4 \times 52\,400 + 0.6 \times 54\,900) \times 1.1$ g/mol = 59 290 g/mol. Wignall et al. [35] determined an empirical law of $\langle R_g^2 \rangle_z = 0.0729$ Å$^2 M_W$ for atactic polystyrene. This calculates 46.7 Å for our parent polystyrene system averaged as $(0.4 \times 29\,800 + 0.6 \times 28\,500) \times 1.03$ g/mol = 29 890 g/mol.

Neither of these estimates for the true θ-dimensions of polystyrene or poly(styrene sulfonate) match our measured chain dimensions, under high salt conditions. Even though both systems are under experimental θ-conditions by displaying the scaling criteria for flexible polymers of $\langle R_g^2 \rangle \sim N$, they may not reflect identical local stiffness

realized in our system, characterized by the characteristic ratio, C_∞ [36].

The degree of polymerization (N) was determined from the value of the intercept to zero angle, via the fit to the Debye structure factor. Although, N is already known, it is important to provide the supporting evidence for the consistency of the high concentration methodology of isotopic labeling for polyelectrolytes. From the general relation for single chain scattering, given in Eq. (18), $I_s(0)$ was determined for all salt concentrations. The data are shown in Fig. 4 where $I_s(0)$ is varying with an average of $2.07 \pm 0.1\ \mathrm{cm}^{-1}$. Using the scattering lengths, polymer concentration, and fraction of protonated chains, from Table 2, we calculate a degree of polymerization of 280, which agrees remarkably well with the isotope-weighted parent polystyrene number and weight average degree of polymerizations of 280 and 287, respectively.

4.2. Total scattering

In addition to the direct measurement of the single chain monomer–monomer correlations, the total scattering was measured. This is achieved by making the prefactor K, in Eq. (18), zero by using a fully protonated polymer in heavy water, $x_h = 1$. The variation in the total scattering is seen in Fig. 5, where the increase in scattering with added salt is clearly seen. The lowest salt concentration corresponding to added salt 0.125 M is sufficiently high such that the expected peak at finite wavevectors [37] is absent.

We quantify the scattered intensity to zero angle, $I(0)$, and the correlation length, ξ, using the Ornstein–Zernicke equation, equivalent to Eq. (10)

$$S_t(\mathbf{q})^{-1} = S_t(0)^{-1}(1 + \xi^2\mathbf{q}^2). \tag{21}$$

The Ornstein–Zernicke plot is shown in Fig. 6, for salt concentrations 0.125, 0.188, 0.250, 0.300, 0.325, and 0.330 M. An incoherent-scattering background of $0.10\ \mathrm{cm}^{-1}$ was subtracted as a flat background from the total scattering data. This is an estimated incoherent background from the protonated NaPSS in D_2O.

Table 2
Experimental quantities

N	0.962 mol/l of solution (2.07×10^{18} polymers/cm^3)
x_h	0.40
y_h	0.33
$v_m(PSS^-)$ [41]	114.8 cm^3/mol
$v_s(H_2O)$ [42]	18.063 cm^3/mol
$v_s(D_2O)$ [42]	18.137 cm^3/mol
b_h(H-PSS$^-$) [43]	47.251 fm
b_d(D-PSS$^-$) [43]	120.124 fm
$b_s(H_2O)$ [43]	−1.675 fm
$b_s(D_2O)$ [43]	19.1458 fm

Upon investigation of the Ornstein–Zernicke plots, one notices the familiar $\mathbf{q}^2$ dependence similar to that observed in neutral polymers as the temperature approaches the critical temperature. Also, it is easily seen that at the lowest wavevectors a significant downturn is apparent, particularly the lower salt concentration data. This deviation (upturn on I versus $\mathbf{q}$, downturn on Ornstein–Zernicke plot) has been observed before for polyelectrolytes [37,38] and neutral polymers [39], with physical interpretation as a form factor for large aggregates. Since we are interested in the monomer–monomer correlations the experimental data fit was away from the strong excess scattering occurring at the lowest $\mathbf{q}$. $I(0)$ and ξ diverge as shown in Figs. 7 and 8, respectively. Data are also shown in Table 3. This divergence becomes significant close to the precipitation phase boundary. ξ increased from 5.0 ± 1.0 to 160 ± 17 Å between

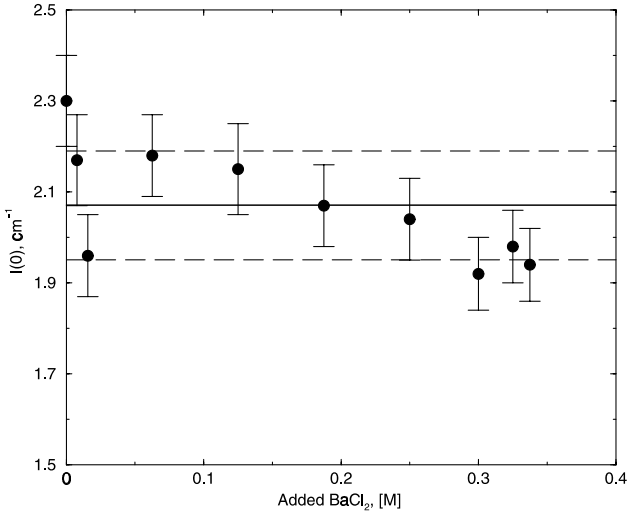

Fig. 4. High concentration labeling, extrapolated scattered intensity to zero angle from fits to the Debye structure factor for 10 different salt concentrations. Average $I_s(0)$ is $2.07 \pm 0.1\ \mathrm{cm}^{-1}$, using experimental parameters given in Table 2, the average calculated degree of polymerization is 280.

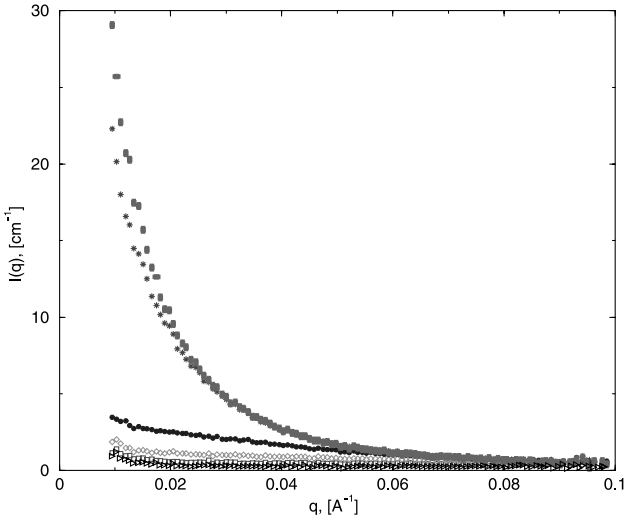

Fig. 5. Total scattering for increasing levels of added barium chloride salt. Legend for barium chloride salt concentration is (▷) 0.125 M, (□) 0.188 M, (◇) 0.250 M, (●) 0.300 M, (∗) 0.325 M, (■) 0.330 M.

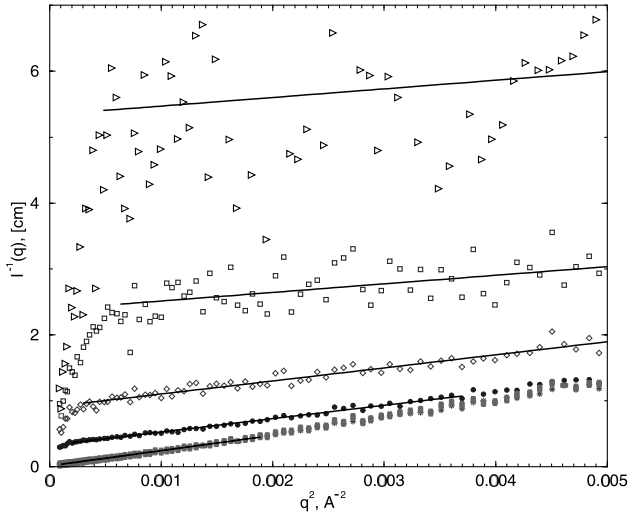

Fig. 6. Ornstein–Zernicke Plot for increasing levels of added barium chloride salt. Legend for barium chloride salt concentration is (▷) 0.125 M, (□) 0.188 M, (◇) 0.250 M, (●) 0.300 M, (∗) 0.325 M, (■) 0.330 M. The excess scattering leading to the downturn is not fit.

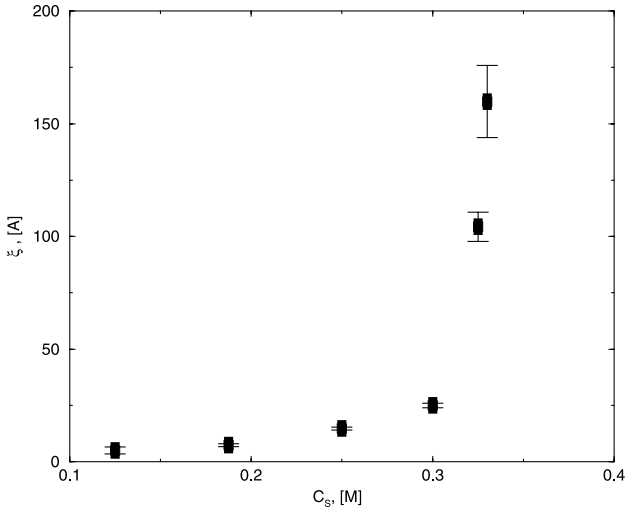

Fig. 8. Total Scattering, correlation length from Ornstein–Zernicke plot as a function of added barium chloride salt concentration.

salt concentrations 0.125 and 0.330 M, respectively. The divergence in $I(0)$ and ξ with increasing salt concentration is similar to that seen for neutral polymer solutions on approach to the spinodal curve by varying temperature. Thus, added salt enhances monomer concentration fluctuations.

4.2.1. Thermodynamic parameters

It was outlined earlier that from the total scattering experiment it is possible to extract the interaction parameters using RPA. Thus, on a plot of $I(0)^{-1}(b^2/v_m) - (1/\phi N) + (1/(1-\phi))$ versus $1/\kappa^2$, shown in Fig. 9, the

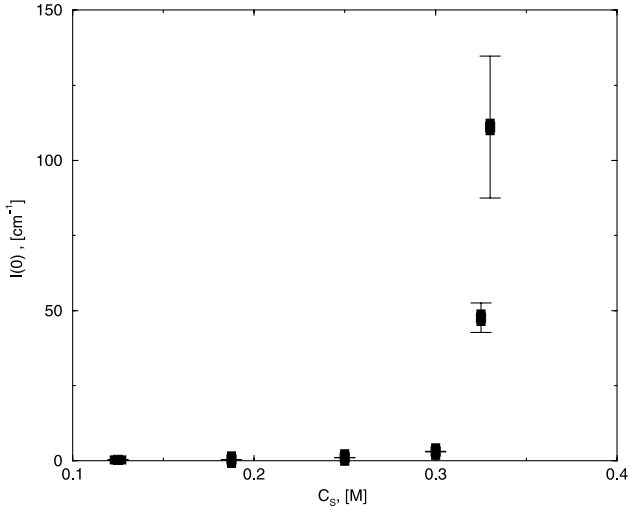

Fig. 7. Total scattering, extrapolated scattered intensity to zero angle from Ornstein–Zernicke plot as a function of added barium chloride salt concentration.

bare χ_0 was experimentally determined to be 1.10 in dimensionless units of energy/k_BT and w_c was found to be 5.57 nm^{-2}.

The expression for the strength of the screened electrostatics, w_c, is Eq. (2). From this, we calculate the monomer degree of ionization, α, to be 0.21, taking the valence of the Kuhn segment $Z = (l_k/a)Z_m$, where monomer valence (Z_m) is unity as dictated by the chemistry and monomeric contour length, a, is 2.3 Å [34]. We take the most recently determined value of the persistence length, l_p, 6.9 Å by Hirose et al. [34] and the Kuhn segment length is twice the intrinsic persistence length, $l_k = 13.8$ Å. Since the theory for the interaction is between Kuhn segments, the proper conversion of valence must be made. This value of $\alpha = 0.21$ was used for all calculations of the Debye length.

In order to determine these thermodynamic parameters properly, they were determined self-consistently, since α is required to input the fraction of counter-ions involved in the screening, quantified by κ^{-1}. This involves performing calculations by comparing the input values of α for the inverse Debye length, κ, and recovered values from w_c.

The value for χ_0 is large and positive, which agrees well for a polyelectrolyte with the hydrophobic backbone. The low degree of ionization calculated agrees well with experimental data, which suggest that the true degree of ionization of a polyelectrolyte is less than the chemical details suggest [4].

Knowing χ_0, we compare it to the Flory–Huggins interaction parameter determined by Beer et al. [4] for flexible polyelectrolytes. To do this, we compare the statistical mechanical calculation for the second virial coefficient between Kuhn statistical segments, l_k, and the second virial coefficient one calculates from the Flory–Huggins χ_0 parameter [3]. The final result is given by Eq. (22). Here, the definition of w and χ_0 are in dimensionless units of

Table 3
Summary of results

C_{salt} (M)	κ^{-1} (Å)	$I_s(0)$ (cm^{-1})	R_g (Å)	$I_t(0)$ (cm^{-1})	ξ (Å)
0	9.57	2.30 ± 0.10	80.3 ± 2.0		
0.0078	8.71	2.17 ± 0.1	80.0 ± 2.0		
0.0156	8.05	1.96 ± 0.09	80.0 ± 2.4		
0.0625	5.87	2.18 ± 0.09	72.6 ± 1.4		
0.125	4.61	2.15 ± 0.10	70.2 ± 1.7	0.187 ± 0.01	5.05 ± 1.5
0.1875	3.92	2.07 ± 0.09	63.6 ± 1.5	0.420 ± 0.021	7.40 ± 0.69
0.250	3.47	2.04 ± 0.09	59.8 ± 1.5	1.10 ± 0.049	14.8 ± 0.64
0.30	3.20	1.92 ± 0.08	55.2 ± 1.2	3.08 ± 0.13	25.0 ± 1.0
0.325	3.09	1.98 ± 0.08	54.2 ± 1.0	47.62 ± 4.9	104.3 ± 6.5
0.330	3.07			111.1 ± 23.6	159.84 ± 17.2
0.3375	3.04	1.94 ± 0.08	54.1 ± 1.0		

energy/k_BT, using $l_k = 13.8$ Å. Using these values, we calculate $w = -0.043$.

$$w = \left(\frac{1}{2} - \chi_0\right)\frac{v_m}{l_k^3}. \quad (22)$$

This value is in disagreement with that reported by Beer et al. [4] for sodium–poly(styrene sulfonate). They found w to be positive and between 0.35 and 0.05. However, our estimate of w leads to a negative value, which is understood that the potential between polymer segments is attractive because of the intrinsic hydrophobic nature of the non-polar styrene monomer, which is trapped in a polar aqueous medium by electrostatics. A negative value for w is recovered by Beer et al. for various quaternized poly(vinyl-pyridine)s. Our estimate of w is close to the proton and ethyl quaternized poly(vinyl pyridine), −0.02 and −0.03, respectively. As these are the closest analogs to NaPSS, the most hydrophobic polymer, benzyl-quaternized poly(vinyl pyridine) value is much greater at −0.32.

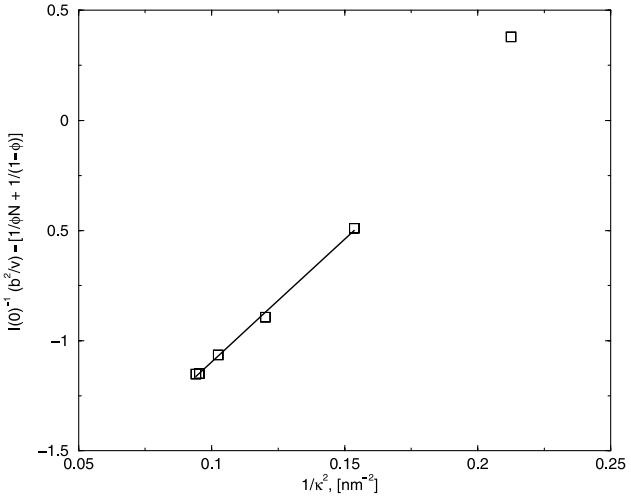

Fig. 9. Thermodynamic plot, details in text. Experimentally determined interaction parameters are $\chi_0 = 1.10$, $w_c = 5.57\ nm^{-2}$. Using known variables $\phi = 0.11$, $N = 280.3$, $l_k = 1.38$ nm, $l_B = 0.715$ nm, $v_m = 114.8\ cm^3$/mol.

Although the degree of quaternization is much lower than the degree of sulfonation, the parallels are qualitatively accurate. It should be emphasized that the comparison we have made are via different theoretical treatments and different experimental conditions. Our experiments are in semi-dilute solution, while Beer et al. are in dilute solution. This theoretical formalism is in the form of examining the isothermal osmotic compressibility, while Beer et al. examine the uniform expansion of isolated chains.

4.2.2. Divergence in ξ and $I(0)$

We have analyzed the divergence of $I(0)$ and ξ in the spirit of the Landau–Ginsburg theory. In a direct analogy for critical phenomena for the divergence of $I(0) \sim \epsilon^{-\gamma}$ and $\xi \sim \epsilon^{-\nu}$, where ϵ is the reduced temperature, $|(T - T_c)/T|$. We present the divergence, not with temperature, but with the solution ionic strength quantified by the square of the inverse-square Debye length, κ^2. κ^2 is given by the experimentally convenient form, Eq. (23) for the 1:2 electrolyte barium chloride and sodium counter-ion. The monomer and salt concentrations, C_m and C_{salt}, respectively, are given in moles per liter of solution.

$$\kappa^2 = 4\pi l_B 1000 N_A(\alpha C_m + 6C_{salt}). \quad (23)$$

As described earlier, plotting ξ^{-2} and $I(0)^{-1}$ versus $1/\kappa^2$, should reveal a straight line with positive slope if the mean-field model is correct. This is precisely what is observed with the experimental data as shown in Figs. 10 and 11. However, a significant deviation is seen at high salt, close to the phase boundary. This deviation signifies the importance of fluctuations, hence, a crossover to the Ising criticality. This concludes that high salt polyelectrolyte solutions are in the same universality class as neutral polymer solutions.

4.3. Coupling of length scales

We have demonstrated the key experimental results of the R_g and ξ variation with added salt. In order to bring some physical insight into the coupling, R_g, ξ, and κ^{-1}

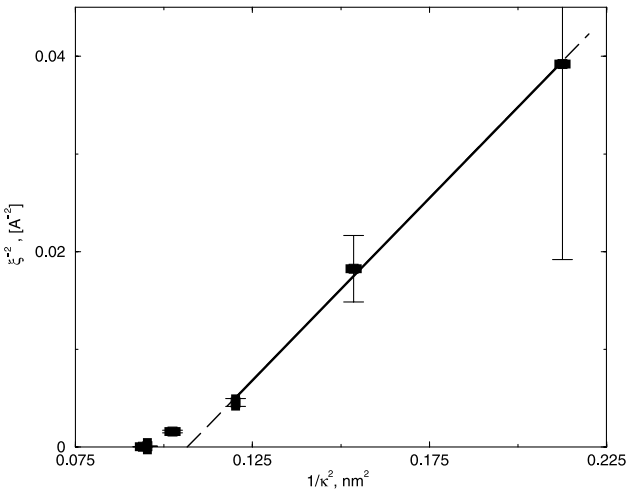

Fig. 10. Demonstration of crossover from mean-field to Ising criticality for ξ^{-2} versus $1/\kappa^2$.

are shown in Fig. 12 with respect to the dimensionless parameter $(\kappa_c^2/\kappa^2 - 1)$. However, the experimental estimate for the critical salt concentration differs by 6.6% between the two types of experiments: 0.335 and 0.357 M for ξ and R_g, respectively. So, the critical κ_c^2 used was 11.38 and 10.773 nm^{-2} for the R_g and ξ experiments, respectively.

Far from the phase boundary the size of the labeled chains is smaller than calculations for rod-like conformations. As argued earlier, this departure from rod-like conformations is consistent with excluded volume screening and electrostatic screening. The excluded volume screening is a result of the semidilute solution nature and the electrostatic screening is provided by dissociated polymer counter-ions. As salt is added to the solution, the radius of gyration decreases. The origin of this decrease is electrostatic in nature and may be theoretically related to the increased electrostatic

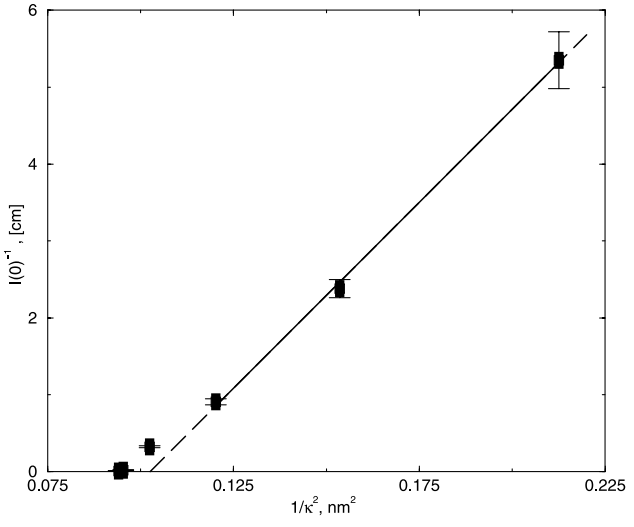

Fig. 11. Demonstration of crossover from mean-field to Ising criticality for $I(0)^{-1}$ versus $1/\kappa^2$.

screening, quantified by the decreasing Debye length, shown as the dashed line. As this electrostatic screening length decreases monomers of the same chain are no longer influenced by the long-ranged Coulombic repulsion. Notice that the magnitude of the Debye screening length is always much less than the radius of gyration and less than the intrinsic persistence length of 6.9 Å. Yet, significant coil contraction is observed. This stresses the importance of electrostatics, even though the calculated theoretical range becomes less than the bare-persistence length of the polymer.

Simultaneously, in the limit of screened electrostatics, the measure of all monomer–monomer correlations ξ is extracted from the experimental data by the Ornstein–Zernicke equation. ξ increases as the phase boundary is approached and begins under low salt as a measure of short-ranged inter-chain correlations [40]. However, as the phase boundary is approached the correlations become longer-ranged due to the diverging behavior with $(\kappa_c^2/\kappa^2 - 1)$. Eventually, the microscopic correlations on the order of the radius of gyration are not important, as the correlation length diverges beyond R_g, such that $\xi \gg R_g$. The crossing of ξ past R_g is observed for critical neutral polymer solutions as the critical temperature is approached. However, in our case the system is not known to be of critical composition, nor approaching a critical point. Even in a complex electrolyte solution similar salient features are observed regarding monomer–monomer correlations, except that the intensive thermodynamic variable tuned is the salt concentration, not temperature.

4.4. θ-Salt calculation

In neutral polymer solutions, a dilute solution may be cooled from the good solvent state, defined where the experimentally measured second virial coefficient (A_2) is large and positive, and maintain the system in an experimentally observable window where $A_2 \approx 0$. This solution is defined as ideal and the solvent quality is referred to as a θ-solvent. From statistical mechanics the second virial coefficient (A_2) may be related to the pseudo-potential or the Flory–Huggins χ-parameter. Thus, the definition of where $A_2 = 0$ can be defined exactly from the molecular details via theoretical calculations,

$$A_2 = 0 = \left(\frac{1}{2} - \chi_{\mathrm{Eff}}\right) = \left[\frac{1}{2} - \left(\chi_0 - \frac{w_c}{\kappa_\theta^2}\right)\right].$$

Thus, it is possible to calculate the expected θ-salt concentration once we know the Flory–Huggins interaction parameter. This can be done most accurately in the high-salt solution limit where the electrostatics is short-ranged leading to a sum of two contributions to short-ranged interactions, a neutral part and electrostatic part as implied by Eq. (5).

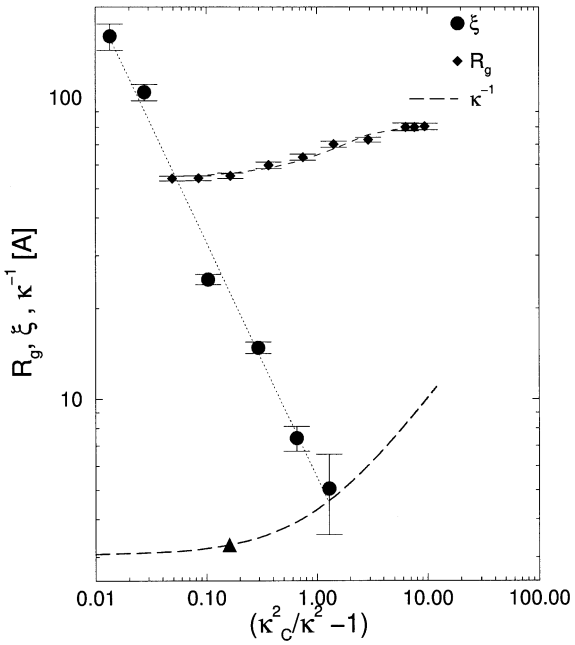

Fig. 12. Composite plot of ξ, R_g, and κ^{-1} versus dimensionless depth from phase boundary. Critical conditions used are $\kappa^2_{c,\xi} = 10.773\ \mathrm{nm}^{-2}$, $\kappa^2_{c,R_g} = 11.38\ \mathrm{nm}^{-2}$. (▲) corresponds to the calculated θ-salt concentration as described in the text.

So, knowing the two parameters χ_0 and w_c, we calculate the θ-salt concentration from κ^2. Then $\kappa^2_\theta = 9.28\ \mathrm{nm}^{-2}$ and the salt concentration corresponds to 0.283 M, this is plotted on Fig. 12 as the (▲) symbol and corresponds to a radius of gyration of 57 Å, which is quantitatively greater than the previously mentions results [34]. This indicates that at least theoretically the polyelectrolyte solution passes into the region of poor solvent quality.

5. Conclusions

We conclude that as barium chloride is added to a semi-dilute solution of sodium–poly(styrene sulfonate) concentration fluctuations are enhanced. This enhancement is due to presence of an unstable precipitation phase boundary. The divergence of the correlation length and scattered intensity to zero angle support the enhancement of concentration fluctuations. The decrease in the single chain dimensions must have electrostatic origin and is explained by electrostatic screening, which increases as the solution ionic strength is increased. The coupling of the Debye screening length to the correlation length and radius of gyration leads to a crossover where $R_g \gg \xi$ to $\xi \gg R_g$. This behavior is similar to that seen in neutral polymer solutions approaching the critical point. In comparison to the mean-field model, the experimental data suggest a crossover from mean-field to Ising criticality, close to the salt-induced phase boundary.

Acknowledgements

The authors are grateful to D. Hoagland and G. Carri for useful discussions. V.M.P. acknowledges the financial support from a National Research Service Award T32 GM08515 from the National Institutes of Health. We acknowledge the sponsored research by the Laboratory Directed Research and Development Program of Oak Ridge National Laboratory, managed by UT-Battelle, LLC, for the US Department of Energy under Contract No. DE-AC05-00OR22725. Acknowledgment is made to NSF Grant No. DMR 9970718.

References

[1] des Cloizeaux J, Jannink G. Polymers in solution, their modelling and structure. New York: Oxford University Press, 1990.
[2] Debye P, Hückel E. Z Phys 1923;24:185.
[3] Muthukumar M. J Chem Phys 1996;105:5183.
[4] Beer M, Schmidt M, Muthukumar M. Macromolecules 1997;30:8375.
[5] Higgins J, Benoit H. Polymers and neutron scattering. New York: Oxford University Press, 1996.
[6] de Gennes PG. Scaling concepts in polymer physics. New York: Cornell University Press, 1979.
[7] Borue VYu, Erukhimovich IYa. Macromolecules 1988;21:3240.
[8] Muthukumar M. In: Baumgärtner A, editor. Molecular basis of polymer networks, vol. 42. New York: Springer, 1989. p. 28.
[9] Joanny JF, Leibler L. J Phys Fr 1990;51:545.
[10] Vilgis TA, Borsali R. Phys Rev A 1991;43:6857.
[11] Olvera de la Cruz M, Belloni L, Delsanti M, Dalbiez JP, Spalla O, Drifford M. J Chem Phys 1995;103:5781.
[12] Chaikin PM, Lubensky TC. Principles of condensed matter physics. Cambridge: Cambridge University Press, 1995.
[13] Williams CE, Nierlich M, Cotton JP, Jannink G, Boue F, Daoud M, Farnoux B, Picot C, de Gennes PG, Rinaudo M, Moan M, Wolf C. J Polym Sci, Polym Lett Ed 1979;17:379.
[14] Akcasu AZ, Summerfield GC, Jahansan SN, Han CC, Kim CY, Yu H. J Polym Sci, Polym Phys Ed 1980;18:863.
[15] King JS, Boyer W, Wignall GD, Ullman R. Macromolecules 1985;18:709.
[16] Melnichenko YB, Wignall GD, Van Hook WA, Szydlowsky J, Wikzura H, Rebelo LP. Macromolecules 1998;31:8436.
[17] Wignall GD, Hendricks RW, Koehler WC, Lin JS, Wai MP, Thomas EL, Stein RS. Polymer 1981;22:886.
[18] Melnichenko YB, Kiran E, Wignall GD, Heath KD, Salaniwal S, Cochran HD, Stamm M. Macromolecules 1999;32:5344.
[19] Nierlich M, Boue F, Lapp A, Oberthur R. Colloid Polym Sci 1985;263:955.
[20] Boue F, Cotton JP, Lapp A, Jannink G. J Chem Phys 1994;101:2562.
[21] Takahashi Y, Matsumoto N, Iio S, Kondo H, Noda I. Langmuir 1999;15:4120.
[22] Spiteri MN, Boue F, Lapp A, Cotton JP. Phys Rev Lett 1996;77:5218.
[23] Wignall GD. Neutron scattering from polymers. In: Grayson M, Kroschwitz J, editors. 2nd ed. Encyclopedia of polymer science and engineering, vol. 10. New York: Wiley, 1987. p. 112.
[24] Vink H. Makromol Chem 1981;182:279.
[25] Smisek DL, Hoagland DA. Macromolecules 1989;22:2270.
[26] Smisek DL. PhD Thesis. Amherst: University of Massachusetts; 1991.
[27] Koehler WC. Physica (Utrecht) 1986;137B:320.
[28] Wignall GD, Bates FS. J Appl Cryst 1986;20:28.
[29] Dubner WS, Schultz JM, Wignall GD. J Appl Cryst 1990;23:469.

[30] Delsanti M, Dalbiez JP, Spalla O, Belloni L, Drifford M. ACS Symp Ser 1994;548:381.
[31] Ikegami A, Imai N. J Polym Sci 1962;62:133.
[32] Axelos M, Mestdagh M, Francoi J. Macromolecules 1994;27:6594.
[33] Narh KA, Keller A. J Polym Sci, Part B: Polym Phys 1993;31:231.
[34] Hirose E, Iwamoto Y, Norisuye T. Macromolecules 1999;32:8629.
[35] Wignall GD, Ballard DGH, Schelten J. J Appl Cryst 1974;7:190.
[36] Strobl G. The physics of polymers. New York: Springer, 1996.
[37] Matsuoka H, Ise N. Adv Polym Sci 1994;114:187.
[38] Ermi B, Amis EJ. Macromolecules 1998;31:7378.
[39] Xie Y, Ludwig KF, Bansil R, Gallagher PD, Cao X, Morales G. Physica A 1996;232:94.
[40] Cotton JP, Nierlich M, Boue F, Daoud M, Farnoux B, Jannink G, Duplessix R, Picot C. J Chem Phys 1976;65:1101.
[41] Ise N, Okubo T. J Am Chem Soc 1968;90:4527.
[42] Lide DR, editor. Handbook of chemistry and physics. 74th ed. Boca Raton: CRC Press Inc., 1993. p. 6–14.
[43] Sears VF. Neutron News 1992;3:26.